Theoretical investigations of models for the laser with a saturable absorber: A case of homoclinic tangency to a periodic orbit

Bruno Zambon
Dipartimento di Fisica, Università degli Studi di Pisa, Piazza Torricelli 2, 56100 Pisa, Italy
(Received 2 April 1990)

A general model for the laser with an intracavity saturable absorber (LSA), with relaxation processes represented by a set of auxiliary variables simply coupled to the field equation, is proposed. Within this framework, a popular model for LSA is discussed through a systematical analysis of the parameter ranges for which chaotic behavior is present. The origin of the instabilities is traced back to the presence of a homoclinic orbit biasymptotic to a periodic unstable solution of the system. The relevant influence of the spontaneous emission in enhancing the underlying deterministic instability is pointed out.

I. INTRODUCTION

When a molecular absorber is placed inside a CO_2 laser cavity, an interesting dynamical behavior is observed, consisting of pulsations and oscillations of the laser output intensity that under some particular conditions may become very irregular and chaotic. Such chaotic pulsations have been reported by many groups involved in the study of laser instabilities as the final step of an intensive search directed towards studying and classifying various kinds of laser dynamical regimes[1-4] and several models based on rate equations have been proposed to explain the rather complex behavior of the laser operating in such configuration.[5-7] Since the early days of laser regime investigations the laser with an intracavity absorber has been termed laser with a saturable absorber (LSA) because highly saturable absorbers were placed into the cavity with the aim of producing very intense and short pulses of the laser intensity. We will adopt in the following this term even if in the majority of the cases in which chaotic behavior is displayed the absorber is no longer subject to such a restrictive condition. The LSA is a very simple nonlinear system; therefore general methods of customary use in the theory of nonlinear dynamical systems have been applied to better characterize and understand its properties. On both sides, i.e., in the experiments and in the numerical simulations, the chaotic signals were analyzed by the use of standard techniques such as power spectrum computation, embedding dimension measurements, and multidimensional attractor reconstruction.[2,4] Furthermore, phase diagrams in the space of laser parameters were computed and determined experimentally to show regions delimiting chaotic and regular behavior.[2,3,7]

The first very general theoretical investigation of LSA was carried out by Salomaa and Stenholm[8(a)] and more recently some attention was paid to this problem, with particular emphasis on the role of the laser frequency on stationary states, by Chyba, Abraham, and Albano.[8(b)] However, in a CO_2 laser the modeling description simplifies to a great extent because a rate equation approach is possible. A step forward in the observation of new regimes and eventually chaos in numerical simulations came as soon as the importance of having different relaxation rates for the upper and lower lasing levels was realized. The role of the fast relaxation of the lower laser level in producing pulses closely similar to those observed experimentally was clearly demonstrated by Tachikawa Tanii, Kajita, and Shimizu.[9] Since then the model of Tachikawa has been used with minor modifications as theoretical support to explain the appearance of chaos in experimental LSA by several groups involved in this research.[4,7,10] However it seems that at the present stage of the LSA investigations a systematic analysis directed towards the identification of meaningful parameters from which the LSA dynamical behavior principally depends becomes necessary in order to facilitate the comparison between experiments and theory. This has not been done in the previous investigations of this system; on the contrary it is evident that the parameters of the numerical simulations were adjusted *ad hoc* to obtain the pulse shapes observed in the experiments. On the other hand, the choice of the parameter values does present some difficulties: beside the fact that some necessary data such as relaxation constants are missing in the literature it is also not trivial to measure independently laser parameters as the total amplification and the saturation power. In light of these considerations one of the purposes of this work will be to carry out an accurate investigation of the ranges of the parameters for which chaotic behavior appears in the rate equations based model which is the best available so far. However, in order to give a more complete theoretical treatment of the LSA dynamics, we will also discuss the mathematical structure of the model which leads to a chaotic dynamics.

It will be shown in this paper that the crucial parameter for the occurrence of chaos in the LSA numerical simulations is the relative saturability of the absorber, i.e., the ratio between the saturation intensity of the amplifier and that of the absorber usually indicated with a: when this parameter is less than unity the region of the control parameters for which chaotic regimes are

present is very wide while this region narrows as a becomes larger than this value. This is, in part, confirmed by the previous numerical simulations on chaotic behavior, in fact, although there is no uniformity on the choice of the system parameters performed by different authors, proper conversions show that they all used values of a which were less than unity. Furthermore, this roughly corresponds to the experimental situations where most of the observations of chaotic regimes are made with high-pressure buffer gas in the absorbing cell, i.e., with high saturation intensities of the absorber. Another important parameter for the LSA behavior is the small signal amplification normalized to the cavity damping of the intensity and usually indicated with A. Concerning this parameter there is a serious discrepancy between experiments and the numerical simulations of the model; what the few direct measurements available[11] provide for the standard CO_2 laser is about one order of magnitude smaller than that needed to obtain chaotic behaviors in numerical simulations. From our investigation we conclude that this model, which apart for minor modifications, is the one adopted in all the numerical simulations of LSA, does not allow us to overcome this difficulty when reasonable values of all the other parameters are adopted.

With regard to the mathematical structure of the LSA equations we will point out the homoclinic nature of the chaotic behavior observed. However contrary to a previous analysis supporting the idea of a homoclinic orbit biasymptotic to an unstable lasing solution[1] we will show that in the LSA this orbit is biasymptotic to an unstable periodic solution of the system. This is indeed the one emerging from the subcritical Hopf bifurcation of the above lasing solution. This distinction is quite important if we think that some properties of the chaotic attractor and of the corresponding chaotic sequences can be determined on the only basis of the invariant set underlying the homoclinic structure. To complete the above analysis we want to emphasize here that the physical mechanism responsible for the presence of the homoclinic behavior is the fast depletion of the lower lasing level which introduces into the mathematical modeling one more variable with respect to the very simple two-level model. This new variable allows a reinjection of the flow in the vicinity of the saddle focus corresponding to the unstable stationary lasing state, not permitted in bidimensional motions, thus providing a close similarity with the case of chemical chaos as in the Belousov-Zhabotinsky reaction or in some thermokinetics models.[12,13]

This work is organized in the following way. In Sec. I we present a general model for the LSA. This model is particularly suited in those situations such as ours in which the internal relaxation structure of the two media is relevant for the dynamical behavior of the system. Here the relaxation degrees of freedom are represented by auxiliary variables simply coupled to the population difference equation. It is of particular importance to provide simple models of the relaxation mechanisms especially in consideration of the relevant improvement obtained in the understanding of the LSA dynamics when the very simple two-level models are abandoned. It is expected that similar improvements could be obtained as well in the analysis of other laser systems. In Sec. II an analysis of the extended model is carried out by focusing on the properties of the stationary solutions; some general properties are discussed and possible differences with respect to the simple two-level system are pointed out. In Sec. III the Tachikawa model is specialized in the formalism of the extended model and a systematic analysis of the LSA regimes it provides is carried out. Here phase diagrams unfolding the chaotic behavior in a bidimensional space of the parameters are presented and discussed, thus allowing us to make considerations on the range of theoretical parameters for which chaotic behavior is to be expected. At the end the nature of the instabilities is discussed and is traced back to the existence of homoclinic orbits biasymptotic to an unstable periodic orbit of the system.

II. THEORETICAL MODELING

A. Basic equations

The set of equations to be used here has already been derived elsewhere and all the approximations involved have been fully discussed.[14] We briefly recall for completeness' sake that the evolution of the intensity of the laser is made in the plane wave and uniform field approximations. The interaction of the field with the medium is ruled by rate equations whose absorption and stimulated emission coefficients are properly modified as an effect of detuning of laser radiation from the atomic transitions. As a consequence of this, the frequency is assumed to be fixed at the cavity frequency and dynamic frequency pulling and pushing effects are considered to be negligible. Both media are treated as homogeneously broadened, which is justified for the passive one because of the high pressure present in the absorbing cell when chaotic behaviors are observed, and only one absorption line is considered to be interacting with the radiation. There are two main differences relative to the set of equations used by other authors. The first one is the inclusion of a noise-source term to account for the spontaneous emission mechanism. This is relevant especially for those regimes characterized by a long permanence of the intensity near the value $I=0$ occurring when the total amplification of the system becomes negative. The failure to include this noise term leads to an incorrect evaluation of the time spent by the system in this lethargic state.[15] The second one is not a substantial difference but just another way to write down the laser equations from which the role of the relaxation mechanisms appear more clearly. If we forget for a moment the spontaneous emission term we can write the LSA equations ruling the evolution of the intracavity intensity I and the population differences in the amplifier and the absorber D and $\bar{D}$ suitably normalized as

$$\dot{I}=-(AD+\bar{A}\,\bar{D}+1)I\ , \tag{1a}$$

$$\dot{D}=-\gamma DI-\int_0^\infty K(t')[D(t-t')+1]dt'\ , \tag{1b}$$

$$\dot{\bar{D}}=-a\bar{\gamma}\bar{D}I-\int_0^\infty \bar{K}(t')[\bar{D}(t-t')-1]dt'\ , \tag{1c}$$

where γ and $\bar{\gamma}$ are given by

$$\gamma=\int_0^\infty K(t')dt, \quad \bar{\gamma}=\int_0^\infty \bar{K}(t')dt \ .$$

Here the time is measured in units of $1/2k$ where k is the damping rate of the electromagnetic (e.m.) field in the cavity. As a consequence of this choice A and $\bar{A}$ are the small signal amplification and absorption constants normalized to $2k$. The intensity is normalized to half of the saturation intensity of the amplifier which in turn is given by

$$I_s=\frac{\gamma}{2B} \ , \tag{2}$$

where B is the stimulated emission coefficient of the amplifier medium. This choice reflects the fact that in the cavity both forward and backward waves interact with the medium, while I is the intensity of only one of them. The memory functions K and $\bar{K}$ represent the effect of collisional mechanisms on the population differences of the amplifier and the absorber. The normalization of D and $\bar{D}$ is transparent from the equations above; D is normalized in such a way as to attain the value -1 in the presence of the pumping mechanism only whereas $\bar{D}$ attains the value 1 at thermodynamical equilibrium. It has been shown that if the relaxation process is represented by a set of linear equations the memory function can be written in the following way:[14]

$$K(t)=c_0\delta(t)+\sum_{i=1}^{n} c_i\gamma_i e^{-\gamma_i t} \ , \tag{3}$$

where δ is the Dirac delta function. It is now clear that although the above form of the laser equations is useful to perform general theoretical considerations it is not practical for numerical simulation purposes. The equations above can be rewritten in terms of a set of auxiliary variables s_i and $\bar{s}_i$, in the following way:

$$\dot{I}=-(AD+\bar{A}\bar{D}+1)I \ , \tag{4a}$$

$$\dot{D}=-\gamma(D+1+DI)-\sum_{i=1}^{n} c_i(s_i-D) \ , \tag{4b}$$

$$\dot{s}_i=-\gamma_i(s_i-D), \quad i=1,n \tag{4c}$$

$$\dot{\bar{D}}=-\bar{\gamma}(\bar{D}-1+a\bar{D}I)-\sum_{i=1}^{\bar{n}} \bar{c}_i(\bar{s}_i-\bar{D}) \ , \tag{4d}$$

$$\dot{\bar{s}}_i=-\bar{\gamma}_i(\bar{s}_i-\bar{D}), \quad i=1,\bar{n} \ . \tag{4e}$$

The equivalence with Eqs. (1) can easily be understood if Eq. (4c) is used to express the auxiliary variables in terms of D. At the end of the transient regime we can write

$$s_i(t)=\gamma_i\int_0^\infty e^{-\gamma_i t'}D(t-t')dt' \tag{5}$$

which when inserted into Eq. (4b) brings it to the original form of Eq. (1b); the same holds for the absorber. There are some advantages in dealing with a set of equations as the ones shown above. The principal one concerns the number of constants that are effectively important in the relaxation process. Normally the relaxation dynamics of the populations of a system of n energy levels requires knowledge of about $n^2/2$ relaxation rate constants; however, not all of them are relevant when our interest is focused on the evolution of the population of only a small number of levels or as in our case on the population difference between two prescribed levels. As it follows from Eqs. (4) only $2n+1$ constants, i.e., the c_i's, γ_i's, and γ, characterize the complete response of the medium. This allows us to point out that in a configuration in which radiation involves only the two energy levels the above constants are the only relaxation parameters whose experimental determination makes sense, and, therefore, their use should be preferred in place of a relaxation schema involving energy levels. In addition, the above form given to the LSA equations is valuable because the other physically relevant parameters such as A and $\bar{A}$ appear directly in the equations in contrast with previous presentations of the model where they had to be computed separately as functions of the various relaxation constants of the two media. This is indeed of some help when a certain region of the physical parameters has to be scanned via numerical simulations of the model. We must also note that the above equations reduce to those of the very simple two-level model in the case when all the c_i's are equal to zero.

B. Adiabatic elimination

There is another situation in which the dynamics of some of the auxiliary variables can be eliminated; this happens when their evolution is very fast compared with the evolution of the principal variables of the system I, D, and $\bar{D}$. Under this condition an adiabatic elimination of the fast variables can be performed. In fact, let us consider Eq. (5), expressing s_i at times where the memory of initial conditions has vanished. We notice that when γ_i is very large as compared with the rate of change of the variable D it is possible to expand $D(t-t')$ around $t'=0$ and integrate, term by term; the result is an approximate expansion for the variable s_i whose first terms read

$$s_i\cong D-\frac{\dot{D}}{\gamma_i}+\cdots \ .$$

It is trivial to verify that when we insert the above expression for the auxiliary variable in Eq. (4b) the net result is a change of the coefficient of $\dot{D}$ in the first member of the equation; this is equivalent to a renormalization of the coefficients γ and of the coupling constants c_k $(k\neq i)$ corresponding to the variables that are not eliminated. The equations of the model therefore maintain their original form except for the appearance of a smaller number of auxiliary variables.

C. Elimination of slow variables

When the rate of change of an auxiliary variable is very slow a stabilization to the average value of D occurs according to Eq. (5), thus allowing us to set it equal to a constant value in the equation for $\dot{D}$. In fact it is expected that its slow and small amplitude fluctuations do not influence the much faster dynamical behavior of D.

D. Determination of coefficients γ_i and c_i

To clarify some technical details of this model we show how the parameters c_i and γ_i can be computed starting from the relaxation scheme of the medium. The procedure consists of a series of linear transformations to set up the variables s_i. First of all in the set of linear equations ruling the population of the levels a transformation is made that introduces D, i.e., the population difference of the levels tuned with the radiation, as a new variable. In a second step the set of equations that does not involve D is viewed as a set of linear equations with external source proportional to D and to a constant term corresponding to the pumping. A linear transformation which diagonalizes and uncouples these equations is then made; this introduces a new set of variables, each one coupled only to D and whose corresponding eigenvalues coincide with our relaxation constants γ_i. An additional scaling and shifting is performed on these new variables to shape their governing equations into the same form of Eq. (4c). The resulting variables coincide now with our auxiliary variables s_i; by expressing the population of each level as a function of s_i and D and inserting the result in the equation for D we will arrive, after an additional normalization, having the purpose to make the equilibrium value of D equal to 1, to Eq. (4b) and consequently to the determination of the coefficients c_i.

E. The four-level model

A short discussion should be given, in the framework of our equations, about a popular model for the CO_2 laser used also in the early modeling of LSA behavior. This model usually known as the four-level model, stems from the peculiar structure of the molecular media, absorber, and amplifier, characterized by a relaxation mechanism involving two lasing or absorbing rotational levels coupled with the corresponding rotational manifolds. In the formalism just introduced two of the three auxiliary variables needed can be eliminated adiabatically due to the very fast rotational relaxations. The third one is extremely slow if the two manifolds relax at the same rate and this is the case when the media can be reduced to equivalent two-level systems. This is indeed the case of previous CO_2 and LSA modeling in which chaotic regimes were not observed.[5] However, when this condition is released by allowing the lower manifold to relax much faster than the upper one, which corresponds to the real situation in CO_2 lasers, the evolution of this variable becomes faster and produces significant modifications to the dynamical behavior of the system. Nevertheless the assumption of equal relaxation times has been widely used to model CO_2 lasers,[16] this being indicative either of the fact that experimental measurements of the laser parameters have never reached the degree of precision necessary to discriminate between several models or that in all experiments the amplifier has never been operated in conditions such as to reveal the presence of the new mechanism. However, experiments on dynamical behavior of the LSA clearly show the necessity to go beyond the simplicity of a two-level model. The model that we will discuss in the following will be based on the key role played by the fast auxiliary variable of the amplifier mentioned above.

III. STATIONARY BEHAVIOR OF THE MODEL

We will examine briefly the properties of the stationary solutions for the general model presented above. A very exhaustive discussion of stationary states' stability has been carried out by Lugiato and co-workers in the framework of a treatment of LSA models with the polarization dynamics in the amplifier and in the absorber.[17] However, the relaxation dynamics considered there is the simplest one and an adiabatical elimination of the polarization, as can be done in CO_2 lasers, leads one to the very simple two-level model without auxiliary variables. We will see that in the extended model some general features concerning stationary solutions and their stability remain unaltered with respect to those already known for the two-level model. However, the auxiliary variables introduce effects such as the modification of the instability windows, and those even more relevant corresponding to the drastic change in the dynamical behavior of the LSA system that will be discussed in the next section.

A. Stationary solutions

It follows from Eqs. (1) that the intensity of the stationary state is governed by the equation

$$I_{\mathrm{st}}\left[\frac{A}{1+I_{\mathrm{st}}}-\frac{\overline{A}}{1+aI_{\mathrm{st}}}-1\right]=0 \tag{6}$$

which allows for a solution $I_{\mathrm{st}}=0$ becoming unstable for $A > A_0=1+\overline{A}$ and a solution different from zero resulting from the second factor. This equation is the same as the one that follows from the two-level model. Figure 1 shows the behavior of the intensity as a function of the amplification parameter A for different values of the relative saturability a, whereas Fig. 2 unfolds the stability regions in the space of the parameters $\overline{A}, A$. The line denoted by HB in the figures corresponds to the Hopf bifurcations of the stationary solution I_+. The situation represented in Fig. 1(c) and also in Figs. 2(b) and 2(c) which corresponds to a bistationary behavior can occur only if $a > (1+\overline{A})/\overline{A}$.

B. Stability of the solutions

To assess the stability of the stationary solutions the dynamics of the small fluctuations must be investigated. This amounts to the determination of the eigenvalues of the matrix L associated with this evolution. It can be shown by simple algebra that the determinant of this matrix does not depend on the coupling coefficients c_i. By indicating with L_R the matrix correspondent to the two-level model we find

$$\mathrm{Det}(L)=\prod_1^n(-\gamma_i)\prod_1^{\bar{n}}(-\overline{\gamma}_i)\mathrm{Det}(L_R)\ ,$$

where $\mathrm{Det}(L_R)$ can easily be determined for the branch of

the nontrivial solutions. It results to be a function of the derivative of the intensity with respect to the parameter A as given by

$$\mathrm{Det}(L_R)=-\gamma\bar{\gamma}I(1+aI_{\mathrm{st}})\left[\frac{dI_{\mathrm{st}}}{dA}\right]^{-1}. \tag{7}$$

Some general properties regarding the stability of the stationary solutions can be deduced from the above expressions and, in particular, from the sign of the determinant of L. The first one is that the branch with negative slope shown in Fig. 1(c) is always unstable because of the existence of at least one positive eigenvalue. The second one is that the loss of stability along a given branch of solutions may occur only via Hopf bifurcation, with the only exception being the limit points.

Let us discuss in the following more in detail the stability criteria for the general model. The peculiar form given to the ruling equations allows one to cast the condition for the stability in an alternate form with respect to that usually given involving the matrix L. If we insert small deviations from the stationary solution $I_{\mathrm{st}}, D_{\mathrm{st}}, \bar{D}_{\mathrm{st}}$ of the form

$$\delta I_{\mathrm{st}}=\delta I e^{\lambda t},\quad \delta D_{\mathrm{st}}=\delta D e^{\lambda t},\quad \delta\bar{D}_{\mathrm{st}}=\delta\bar{D}e^{\lambda t}$$

into Eqs. (4), we arrive after very simple calculations to a self-consistency requirement which can be stated as

$$\mathrm{Det}\begin{vmatrix} -\lambda & -AI_{\mathrm{st}} & -\bar{A}I_{\mathrm{st}} \\ -\gamma D_{\mathrm{st}} & -\Gamma-\lambda & 0 \\ -a\bar{\gamma}\bar{D}_{\mathrm{st}} & 0 & -\bar{\Gamma}-\lambda \end{vmatrix}=0\,, \tag{8}$$

where Γ and $\bar{\Gamma}$ are given by

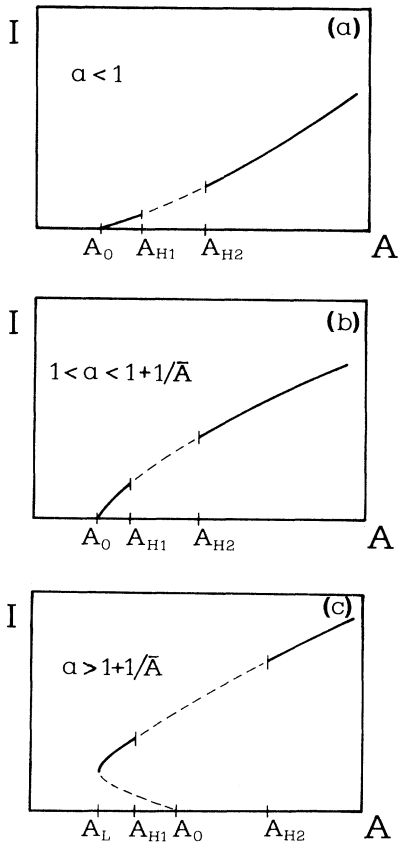

FIG. 1. Stationary laser intensity vs A for different conditions regarding the saturation parameter a. (a) Saturation intensity of the absorber bigger than that of the amplifier ($a<1$); (b) $a>1$ with monostationary behavior; (c) $a>1$ with bistationary behavior. The dotted portion of the branch corresponds to the unstable window between two Hopf bifurcations A_{H1} and A_{H2}. We remark that (c) shows a pathological case because for realistic parameter values there is no Hopf bifurcation corresponding to A_{H1}.

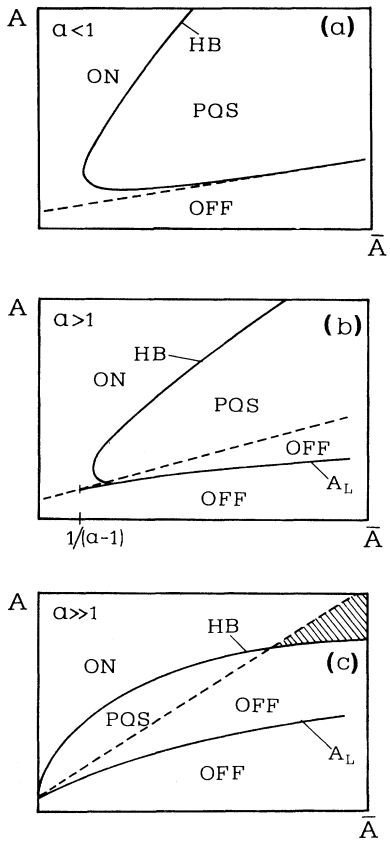

FIG. 2. Unfolding in the space $\bar{A}, A$ of the stability domains. HB is the Hopf-bifurcation line, A_0 (dashed line in the figures) represents the threshold for laser oscillations, and A_L the line corresponding to the limit point of the branch of stationary solutions. The branch becomes bistationary for $\bar{A}>1/(a-1)$, as can be seen in (b) and (c). For $a\gg 1$ bistability occurs in the hatched area in (c). The region where only time-dependent regimes are possible is denoted by PQS. We point out that the pattern of the HB shown in (b) near the confluence of the A_0 and A_L lines has been extremely magnified to show its general behavior. In practice, for realistic parameters, the HB line joins the A_0 and A_L at their confluence.

$$\Gamma(\lambda)=\gamma(1+I_{\rm st})-\sum_{i=1}^{n}\frac{c_i\lambda}{\lambda+\gamma_i}\ ,$$
$$\overline{\Gamma}(\lambda)=\overline{\gamma}(1+aI_{\rm st})-\sum_{i=1}^{\bar{n}}\frac{\bar{c}_i\lambda}{\lambda+\overline{\gamma}_i}\ . \tag{9}$$

It must be noticed that the zeros of the two functions above correspond to the eigenvalues $-\beta_i$ and $-\bar{\beta}_i$ of the relaxation processes represented, respectively, by Eqs. (1b) and (1c) when the intensity is kept fixed to the value $I_{\rm st}$; this means that their real part must be negative. It may be useful to express Γ and $\overline{\Gamma}$ in the following way:

$$\frac{1}{\Gamma+\lambda}=\sum_{i=1}^{n}\frac{\alpha_i}{\lambda+\beta_i}\quad\frac{1}{\overline{\Gamma}+\lambda}=\sum_{i=1}^{\bar{n}}\frac{\bar{\alpha}_i}{\lambda+\bar{\beta}_i}\ ,$$

which holds if the eigenvalues are not degenerate. If we transform the condition expressed by Eq. (8) we obtain

$$\lambda=-\gamma I_{\rm st}\frac{A}{1+I_{\rm st}}\frac{1}{\Gamma+\lambda}+\overline{\gamma}I_{\rm st}\frac{a\overline{A}}{1+aI_{\rm st}}\frac{1}{\overline{\Gamma}+\lambda} \tag{10}$$

which is a general expression that can be used to compute the eigenvalues associated with the stationary solutions of the system. Once the c_i and γ_i are known, the above equation may provide useful insight into the position of the eigenvalues just be a simple graphical inspection; this may sometimes be a better and more intuitive approach than the diagonalization of L, which makes direct use of the relaxation constants between energy levels.

C. Stability for small intensities (near the threshold)

As an application of the above equation we will determine the stability properties of the solutions near $I_{\rm st}=0$. In this case the second member of Eq. (10) is very small except for the point where $1/(\Gamma+\lambda)$ and $1/(\overline{\Gamma}+\lambda)$ become singular. This means that the values of λ satisfying this equation will be with good approximation equal to $-\beta_i$ and $-\bar{\beta}_i$. The remaining eigenvalue will be close to zero and can be obtained by power expanding the second member of Eq. (10) around $\lambda=0$. By carrying out the simple calculation we find

$$\lambda\cong-I_{\rm st}\left[\frac{dI_{\rm st}}{dA}\right]^{-1}\ , \tag{11}$$

telling us that in the neighborhood of the threshold the branch with the negative slope has only one positive eigenvalue whereas the branch with positive slope is stable.

An additional result on the stability near threshold can be obtained if we observe that γ is usually a very small quantity, thereby introducing a slow time scale in the dynamics of the system. An interesting situation arises when this becomes comparable with that defined by the eigenvalue λ computed above. To make our arguments more precise we will assume, in accordance with the model to be discussed in the next section, that the absorber and the amplifier do not have slow auxiliary variables and that $\overline{\gamma}\gg\gamma$. In this hypothesis, and by assuming that $\lambda\ll\gamma_i$, Eq. (10) is transformed into

$$\lambda=-\tilde{\gamma}A\frac{I_{\rm st}}{1+I_{\rm st}}\frac{1}{\tilde{\gamma}(1+I_{\rm st})+\lambda}+\overline{A}\frac{aI_{\rm st}}{(1+aI_{\rm st})^2}\ , \tag{12}$$

where we have set

$$\tilde{\gamma}=\gamma\Big/\left[1-\sum_{1}^{n}\frac{c_i}{\gamma_i}\right]\ ,$$

which by virtue of some properties of the coefficients c_i and γ_i is always greater than zero. This result coincides with the stability equation of the two-level model whenever γ is replaced by $\tilde{\gamma}$. It is instructive to carry out the calculations because related situations have been reproduced in LSA experiments.[18] By simple algebraic manipulations we can put Eq. (12) into the following form:

$$\lambda^2+\lambda\left[\tilde{\gamma}(1+I_{\rm st})-\overline{A}\frac{aI_{\rm st}}{(1+aI_{\rm st})^2}\right]+\tilde{\gamma}I_{\rm st}\left[\frac{dI_{\rm st}}{dA}\right]^{-1}=0\ ,$$

which allows us to characterize analytically the behavior near threshold. Let us assume the monostationarity condition $a<(1+\overline{A})/\overline{A}$ so that $dI_{\rm st}/dA>0$. In this case a Hopf bifurcation occurs when

$$\frac{\tilde{\gamma}}{a\overline{A}}=\frac{I_{\rm st}}{(1+I_{\rm st})(1+aI_{\rm st})^2}\ . \tag{13}$$

The two values of the intensity which solve this equation correspond to the window of instability between A_{H1} and A_{H2} of Fig. 1(a). The equation above shows that A_{H1}, which is known from numerical analysis to correspond to a supercritical Hopf bifurcation, occurs at growing intensities as a becomes smaller. However, in normal conditions A_{H1} is very close to the threshold so that the corresponding transition is always buried by the noise of the system. The addition of a buffer gas in the absorbing cell of the LSA allows an increase of this last parameter by a sizable amount, thus the observation of stable sinusoidal modulation emerging from A_{H1} becomes possible.[18]

D. Properties of the coefficients c_i and γ_i

We are unable at present to provide a more complete discussion of the stability on the basis of Eq. (10) without going through an explicit evaluation of the coupling and damping coefficients c_i and γ_i. Although these are related, via the procedure outlined in Sec. II D, to relaxation processes that are Markovian and that are very well characterized in all their mathematical properties, the search for general properties involving them and relevant to the solution of Eq. (10) seems at first glance difficult to carry out. The only property we have been able to determine so far is the sign of $\tilde{\gamma}$, which was mentioned above. However, we can make additional comments regarding the peculiarity of the relaxation process resulting from the combined action of the pumping mechanism and collisional relaxations as in the active medium of the laser; here in fact the detailed balance condition is no longer satisfied, thus allowing the possibility that γ_i and/or β_i be complex numbers.[19] Although in our numerical calculations we have always found real coefficients we cannot exclude the fact that for some range of the parame-

ters complex values appear; in this case the dynamical behavior of the laser system would be enriched by the presence of the intrinsic frequency corresponding to the imaginary part of these eigenvalues. It is not clear now how much this can be of relevance (and we plan to investigate it in a future work), to the presence of LSA regimes not reproducible with a three-dimensional model as, for example, just to mention one, the appearance of breathing oscillations.[7] However, it appears interesting that at least in principle this situation may arise in a laser system. Another correlated question concerns possible instabilities of the laser oscillations. In the very-well-known Lorenz-Haken[20] model the instabilities arise because of the key role played by the polarization of the medium, whereas the relaxation scheme is chosen to be the simplest one. Instabilities in which the polarization is adiabatically eliminated but the relaxation is considered in all its complexity has never been studied nor been observed experimentally in pure laser systems. However, it would be interesting to prove either that they can be ruled out on the basis of well-established properties of a Markovian relaxation process as the one used to model the active medium, or that they are allowed to occur, even if the laser parameters would result in being outside normal ranges.

E. Eigenvalues

We now give a picture of how the eigenvalues behave as we move along the branch of stationary solutions. We begin this discussion with an analysis of the one auxiliary variable model in a range of parameters fitted for CO_2 LSA and only hint at possible modifications induced by a more complex modeling of the relaxations.

Let us consider first the bistationary case; by starting at the point $I_{st}=0$ and moving along the branch of stationary solutions we encounter first an unstable portion of the branch which may extend beyond the limit point. In this case, which usually occurs for low values of a, another positive eigenvalue joins, at the crossing of the limit point, the already existing one in such a way that in the branch with positive slope two positive eigenvalues are found to exist. These, as we move further beyond the limit point, collide and transform into a pair of complex conjugate eigenvalues whose real part crosses the real axis at the point where the inverse Hopf bifurcation A_{H2} occurs. In the other case, which usually occurs for very high values of a, at the crossing of the limit point the only negative eigenvalue becomes positive and the solution becomes stable from this point onward. The appearance of a window corresponding to Hopf bifurcations as shown in Fig. 1(c) occurs in an extremely tiny region of LSA parameters to be practically undetectable. In fact, this situation originates at the transition from monostationary to bistationary behavior where a stability pattern like that of Fig. 1(b) transforms into that of Fig. 1(c); this occurs when a is of the order of unity and the level of the intensity corresponding to A_{H1} is very low to be experimentally detectable. The situation for the extended model depends on the properties of the relaxation parameters c_i and γ_i for both the amplifier and the absorber. We may reasonably expect that additional pairs of complex conjugate eigenvalues appear and disappear as we move along the branch of stationary solutions. The interesting question here is if the real part of these pairs may ever become positive; we would assist in this case to the presence of more branches of periodic solution stemming from the corresponding Hopf bifurcations. The relevance of this to the dynamical behavior of the system is rather evident; the presence of more branches could lead to generalized bistability and increased possibilities of irregular behavior.

The case of monostationary behavior is depicted in Figs. 1(a) and 1(b). Figure 2(a) shows the ranges of the stable and unstable solutions in the plane $(\overline{A}, A)$. As it has emerged from the analytical discussion presented above the part of the branch immediately near to $I_{st}=0$ is always stable; by moving further along the direction $\overline{A}=$const the solution may lose its stability via a Hopf bifurcation and regain it again via an inverse Hopf bifurcation. Also here additional pairs of complex conjugates eigenvalues with positive real parts may be possible in principle.

IV. ONE AUXILIARY VARIABLE MODEL

We will carry out a systematic analysis of a model equivalent to the one introduced first in the study of the LSA by Tachikawa and co-workers.[9] Extensive simulation work has been done in the past by Mandel and Erneux for a two-level model of the LSA including polarization both in the amplifier and in the absorber.[21] However, at that time chaos had not yet been observed in the experiments and momentum for a theoretical search of chaotic regimes was not high. Furthermore in CO_2 lasers polarization is eliminated adiabatically and the relaxation structure needed to find chaos was not present in the model there described.

A. The ruling equations

In this model we introduce an auxiliary variable in the amplifier corresponding to its peculiar internal relaxation process. The absorber in the model is represented by a two-level system; this may be a satisfactory representation for some infrared absorbers but not for others as, for example, SF_6 where the hot-band mechanism of absorption is well known.[22] However, in the high-pressure range in which we are interested it is not yet clear if this will produce relevant changes in the behavior of the system. Furthermore in these operating conditions an adiabatic elimination yields an intensity-dependent absorption coefficient for this medium. The LSA equations for our model then read

$$\begin{aligned}
\dot{E} &= -\frac{1}{2}\left[AD+\frac{\overline{A}}{1+a|E|^2}+1\right]E+\xi(t)\ , \\
\dot{D} &= -\gamma(D+1+D|E|^2)-c_1(s-D)\ , \\
\dot{s} &= -\gamma_1(s-D)\ ,
\end{aligned} \tag{14}$$

where E is the complex field amplitude normalized to

$1/\sqrt{2}$ the saturation value in the amplifier, and $\xi(t)$ is a complex white Gaussian process representing mainly, in CO_2 lasers, the effect of spontaneous emission. This term as well as the very simple form of the LSA equations were not present in the original formulation of the model.[9] The properties of the noise are given by

$$\langle \xi_i(t)\xi_j(t')\rangle = 2Q\delta_{ij}\delta(t-t') ,$$

where $i,j=1,2$ for the real and imaginary parts. The strength Q of the noise can be determined by a very simple argument[23] that can trivially be extended to the LSA. At thermal equilibrium the e.m. field is represented by an Ornstein-Uhlenbeck process given by

$$\dot{E} = -\tfrac{1}{2}[A(M_1-M_2)+\overline{A}(\overline{M}_1-\overline{M}_2)+1]E+\xi(t) ,$$

where the population $M_1, M_2, \overline{M}_1, \overline{M}_2$ stands for the average value of the populations of the lasing and absorbing levels, respectively. Fluctuations of these last variables due to collisions are negligible and so are the fluctuations produced on them by the field. The thermal equilibrium value of $|E|^2$ is given by

$$\langle |E|^2\rangle_{\rm th} = \frac{4Q}{A(M_1-M_2)+\overline{A}(\overline{M}_1-\overline{M}_2)+1} = \frac{2n_{\rm th}}{n_{\rm sat}} ,$$

where $n_{\rm th}$ is the thermal equilibrium photon occupation number and $n_{\rm sat}$ is the number of photons in the mode corresponding to the saturation intensity. By solving with respect to Q in a thermal equilibrium situation we find

$$Q = \frac{1}{2n_{\rm sat}}(AM_2+\overline{A}\overline{M}_2+1) , \tag{15}$$

where M_2 and $\overline{M}_2$ are normalized in the same way as D and $\overline{D}$. The validity of the above equation extends as well outside the ranges of a thermal equilibrium situation. In our computations we will assume, for reasons of simplicity, that Q is constant and equal to the value at the threshold because we do not expect drastic changes with respect to the use of Eq. (15) and because experimental measurements are not at the stage where one can appreciate such a difference in the model. The numerical simulations of the above equations have been carried out by means of a numerical integrator of the Runge-Kutta type truncated to the fourth order with variable time steps such that the relative error at each step be less than 10^{-4}. The noise has been included in a standard way and some technical artifices have been adopted to cut down the long computation time required, in some cases, by the integrator near $I=0$. With regard to the values of the parameters to be used in our simulations it has already been shown that γ_1 and c_1 are simply related to the fast relaxation rate of the lower laser level.[14] The damping γ can be determined via Eq. (2) from the saturation intensity of the amplifier. By doing so reasonable values for our normalized parameters result to be

$$\gamma = 1.6\times 10^{-3}, \quad \gamma_1 = -c_1 = 0.1, \quad Q = 10^{-12} .$$

B. Classification of the dynamical regimes

Different types of regimes characterized by spikes or modulation of the laser intensity are found to exist by solving numerically the LSA equations. If chaos is not present they are periodic and a suitable classification can be carried out.[7] The most common among the LSA regimes is the widely known passive Q-switching (PQS) regime characterized by sharp spikes followed by long periods where the intensity attains the noise level. A different temporal behavior is displayed by pulses having a main spike which decays to zero through a ringing tail. According to the number n of oscillations in the tail these regimes can be termed as $P^{(n)}$ regimes. The normal PQS pulse in this classification scheme will be denoted by $P^{(0)}$. The existence of the pulses $P^{(n)}$ with $n>0$ is related to the particular structure of the space of the system variables and, in particular, to the presence of a stationary point I_+ with a saddle focus instability; the oscillations in the tail of the pulses are the result of an outward spiraling motion of the system in the unstable manifold of this point; a reinjection of the system flow in the vicinity of this same point then completes the cycle. Some attention has been paid in the past to ascertain if the strong attractive eigendirection is by itself sufficient to provide the reinjection mechanism; we want to show here that although this is a very appealing possibility it is not supported by numerical calculations. In fact, in this model the existence of the strong attractive eigenvalue of I_+ (λ_+) mirrors the fast relaxation rate of the lower lasing level; however, if this is too fast the equations become those of a two-dimensional model by virtue of the adiabatic elimination and the orbits $P^{(n)}$ then disappear thus forcing the conclusion that the strong attraction exerted by I_+ is not sufficient to provide the existence of these regimes. This leads us to consider also the strong attracting eigenvalue of I_0 (λ_0) and to acknowledge that the $P^{(n)}$ regime may result from a proper balance of these two actions. However, a possible way to do it in a quantitative fashion is to consider the ratio of these two eigenvalues and to see whether this can suggest a valid criterion for the existence of the $P^{(n)}$ regimes. Figure 3 shows this ra-

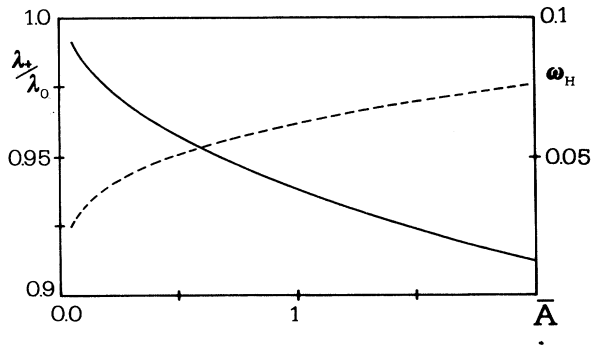

FIG. 3. The ratio between the attracting eigenvalue of I_+ (λ_+) and the attracting eigenvalue of I_0 (λ_0), solid line, and frequency ω_H of the pair of complex conjugate eigenvalues of I_+, dashed line at the point A_{H2} for $a=0.3$ and the other parameters in the text. All quantities are normalized to $2k$.

tio when we move along the line corresponding to the Hopf bifurcation A_{H2} in the space $\overline{A}, A$. The monotonic behavior of λ_+/λ_0 displayed in this figure does not account for the fact that $P^{(n)}$ regimes appear for a certain range of values of $\overline{A}$, as will be shown later in Sec. IV D. Aside from the validity of the above arguments which do not consider the presence of other attractors present in the system such as, for example, stable manifolds of periodic orbits, we can draw the conclusion that the relation of local structure with global behavior is usually a very weak one. In fact it will be found that the $P^{(n)}$ regimes must be traced back to the existence of a homoclinic reinjection in the neighborhood of the point I_+ which is a global property of the flow and cannot be decided on the basis of local properties as the relative strength of the eigenvalues.

In addition to the class of pulses described above, almost sinusiodal modulations of the laser intensity, never reaching the noise level, are observed; these will be named T regimes. They belong to a branch of periodic solutions that originate from a Hopf bifurcation which is supercritical and therefore leading to stable oscillations numerically observed in the range of less than unity; this experimentally corresponds to a high pressure in the absorbing cell. It is interesting to note that by varying the LSA parameters a T pulse can transform continuously into $P^{(0)}$ or PQS pulses. In the following the terms T, $P^{(0)}$, and PQS will be used interchangeably depending on the cases because they pertain to the same branch of periodic solutions.

C. The branch of periodic solutions

Our understanding of the dynamical behavior of a nonlinear system can be greatly improved if we analyze the branch of periodic orbits in support of the numerical simulations. In fact it is clear that such orbits are much better indicators, although never complete ones, of the global behavior of the system than stationary solutions. A similar analysis has been carried out for the optically pumped molecular laser equations by using a dedicated bifurcation software package.[24] There exists also some results for the LSA but not for parameters where a chaotic behavior is found[25]. We will try to extend these results, without explicitly performing the computation of the branches, on the basis of our study of the regions of the existence of different regimes in the phase space $\overline{A}, A$.

The most common scenario for the LSA is depicted in Fig. 4. The branch of periodic solutions starts from a subcritical Hopf bifurcation of the stationary solution I_+ leading to an unstable regime of the T type. As A increases the amplitude of these oscillations increase and their shape deforms continuously to that of a PQS pulse. Independently of how fast this transformation takes place, for our convenience, we will refer to the upper part of the branch after the the limit point A_T as the PQS branch and to the lower part of the branch as the T branch. As A is decreased the PQS solution can be transformed into a cycle of a very long period, Fig. 4(a), or collapse into a stationary solution via an inverse Hopf bifurcation, Fig. 4(b). We note that in the case of the

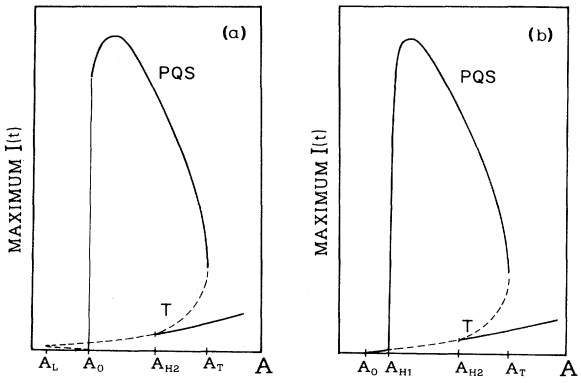

FIG. 4. Shown are the branchs of the stationary and periodic solutions. This last one emerges from the Hopf-bifurcation point A_{H2} and is represented in the figure by the maximum of the corresponding periodic solution. Solid and dotted lines represent stable and unstable solutions. In the case shown here these branches coincide, respectively, with the PQS and T branches, however, in general, the PQS branch may not be stable. In the bistationary case (a) the PQS branch ends with a cycle of a very long period as we approach A_0, while in the monostationary case (b) it undergoes an inverse Hopf bifurcation in A_{H1}. The figures shown here are only sketches of the LSA behavior, therefore, no numerical values appear on the y axis.

two-dimensional (2D) model, if a subcritical Hopf bifurcation occurs as in the point A_{H2} of Fig. 4, the PQS branch is always stable while the T branch is unstable and the limit point corresponds to the coalescence of the two orbits; furthermore the unstable manifold of the T orbit coincides with the stable manifold of the PQS orbit. However, for topological reasons, the two-dimensional model does not allow the presence of a ringing tail observed experimentally so that a more complete model must be considered, by doing so also the PQS solution may become unstable. In this case the orbit leaving the PQS pulse can be attracted by the stable manifold of the T pulse or by that of the I_+ solution and return to the PQS solution via the unstable manifold; this gives rise to a quasiheteroclinic behavior. However, it is clear that this does not imply the presence of an heteroclinic orbit; as a matter of fact we will report in the next sections on the presence of a homoclinic orbit biasymptotic to the T solution and responsible for the $P^{(n)}$ regimes. On the other hand it is quite clear that the reinjection mechanism of these regimes is somewhat correlated to the presence of a PQS unstable orbit.

The scenario described above can lead to bistability between periodic solutions or between a stationary solution and periodic ones as can be seen in Fig. 4; this is known as generalized bistability. In the simplest case we have bistability between PQS and I_+ as shown in Fig. 4; however, a more complex situation may occur when the PQS branch becomes unstable by allowing bistability also with chaotic regimes. The hysteresis cycle then resulting is delimited from one side by A_{H2} and by the other side by a value of $A = A_T$ that we will name transition value or

transition point (TP). In the space $\bar{A}, A$ the set of these points defines a line that we call transition line (TL). It is very important to notice in light of the above discussion, that the transition point, i.e., that point where the dynamic regime collapses on I_+, does not necessarily coincide with the limit point of the periodic solutions branch.

D. Search for chaotic regimes

We have performed a systematic search of chaotic regimes with the purpose of identifying regions of the parameters for the occurrence of chaos in this model. Indeed we have noticed that chaos is always found to be contiguous to the TL line. When $a < 1$ the regions of chaos are very wide and easily detectable whereas, when a becomes larger than unity, these regions gradually disappear until for $a \cong 20$ no sign of irregular behavior exists and only the $P^{(0)}$ regime is present, Fig. 5. The above behavior depends weakly on the values of the parameters γ, and $\gamma_1 = -c_1$ but the role of a is by far the more marked. Of course when $\gamma_1 = -c_1$ increases adiabatical elimination can be applied; the model then transforms into a two-dimensional one and the possibilities to observe chaos vanishes.

We point out here that, since the system we are dealing with is not purely deterministic because of the presence of the spontaneous emission term, we cannot speak strictly of deterministic chaos. On the other hand the exclusion of the noise term would lead to a very unrealistic LSA model not deserving of being studied. However it must be noticed that this noise is very small and its influence is important only in those regimes in which the laser completely turns off; this is the rule when $a > 1$ whereas for $a < 1$ these regimes occur when we move with the parameters A and $\bar{A}$ far away from the TL line. In this last case, the chaotic regimes detected near the transition line are truly deterministic.

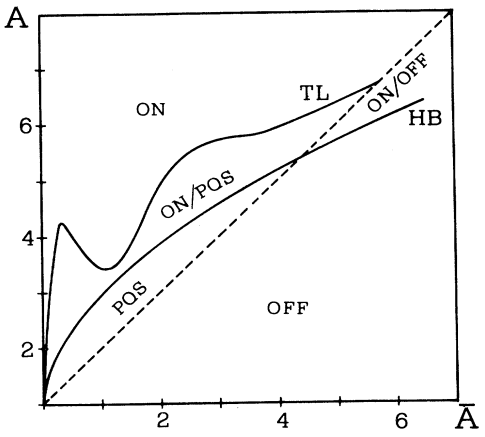

FIG. 5. Unfolding in the space $\bar{A}, A$ of the stability domains of the LSA for the case $a = 50$ and the other parameters in the text. We observe bistability of I_+ with $P^{(0)}$ (ON/PQS) in the region between HB and TL lines and of I_+ with I_0 (ON/OFF) between the HB line and A_0 dashed line. No signs of chaotic behavior are present.

For $a > 1$ the structure of the chaotic signal is recognizable as a random sequence of pulses of the $P^{(n)}$ type with different n. Figures 6(a) and 6(b) show a phase diagram delimiting the regions of existence of different regimes. It appears that in some cases transitions $P^{(n)} \rightarrow P^{(n+1)}$ occur sharply and in others they occur gradually through a region in which a random sequence of $P^{(n)}$ and $P^{(n+1)}$ exists. From Fig. 6(b) we can observe that the regions corresponding to a pure $P^{(n)}$ regime become smaller and smaller as n increases suggesting the presence of a limiting very unstable flow. These regions are surrounded by others characterized by a spread and an average value of n which increases as we move towards the transition line. As pointed out above we must control the effect of the noise on this behavior by replacing the random noise with its equivalent deterministic spontaneous emission term; by doing so the erratic evolution disappears and sharp transitions characterize the passage from $P^{(n)}$ to $P^{(n+1)}$. This suggests that even if

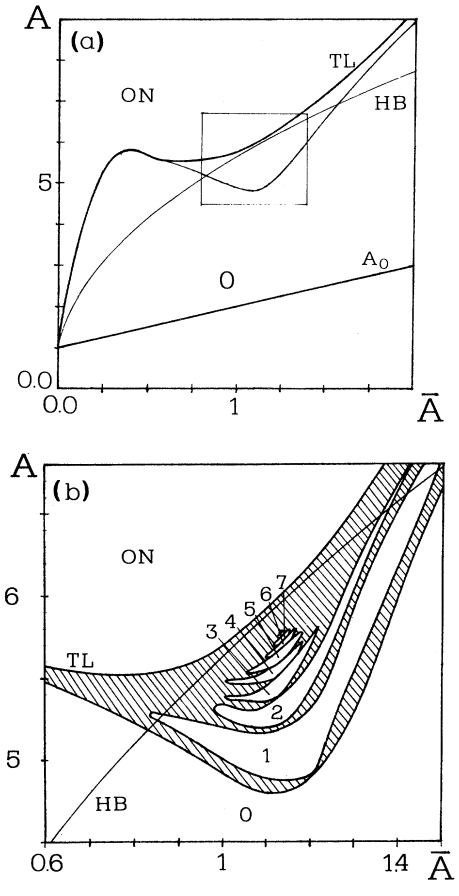

FIG. 6. State diagram of LSA in the space $\bar{A}, A$ for $a = 10$. (a) Overall view; (b) enlargement of the inset in (a). Regimes corresponding to a random sequence of pulses $P^{(n)}$ with different n, named hesitations in Ref. 1, occur in the hatched area. The regions of pure $P^{(n)}$ are indicated by the number n and are separated by regimes corresponding to a mixture of the two adjacent $P^{(n)}$ and $P^{(n+1)}$; however, far from this bordering area mixtures with more than two $P^{(n)}$ exist.

the deterministic chaos does not show up a potentially unstable deterministic situation where even a small microscopic noise can provoke a macroscopic effect must exist. We discuss in the following the origin of this potentially unstable situation.

In the LSA the peculiar shape of the $P^{(n)}$ pulses suggests that at the basis of the unstable behavior observed there should be a homoclinic orbit whose nature, on the other hand, has never been fully established. In some of the previous investigations of the LSA dynamics it was suggested that this orbit should be biasymptotic to the stationary point I_+. However, this does not seem to be the case here; if it would be so $3D$ portraits of the system orbits would show an approach toward point I_+ along its stable manifold, which does not appear, for example, from Figs. 7(a) and 7(b); furthermore chaotic behavior would cease when I_+ becomes stable and this does not occur either, as can be seen in Figs. 6(b) and 9(b). As a matter of fact another possibility can be considered, i.e., the presence of a homoclinic orbit biasymptotic to a periodic unstable orbit of the system having an instability

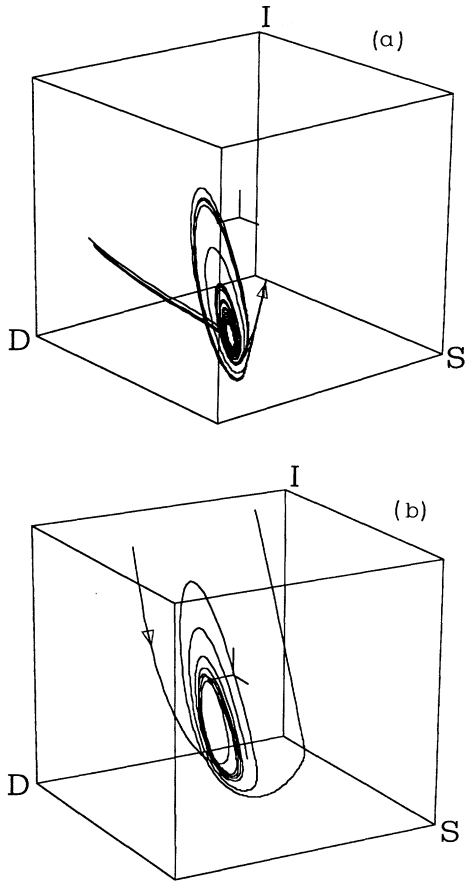

FIG. 7. Three-dimensional view of the LSA orbits. Parameters and value ranges are (a) $\bar{A}=1.1$, $A=5.7$, $a=10$, $\gamma_1=-c_1=0.1$, $\gamma=1.6\times10^{-3}$; $D=S=(-0.25,-0.15)$, $I=(0,20)$; (b) $\bar{A}=2.16$, $A=12.0$, $a=0.66$, $\gamma_1=-c_1=0.14$, $\gamma=2.3\times10^{-2}$. $D=S=(-0.3,0.0)$, $I=(0,25)$. The reinjection orbits are visible in both cases.

of saddle type, this orbit being just the one emerging from the Hopf bifurcation of I_+. The qualitative difference between the first and the second case is that whereas in the first the approach to the neighborhood of I_+ takes place in a direction tangent to the stable manifold of this point identified by the attractive eigenvector, in the latter the approach occurs almost transversally; in the limit case of this transversal approach the structurally unstable homoclinic orbit results exactly tangent to the stable manifold of the unstable periodic orbit. Homoclinic orbits to an invariant set of saddle type other than a point, as is the case of the first Shil'nikov theorem,[26] have been treated by Shil'nikov himself to generalize the previous results.[27] Gaspard and Wang have discussed quite in detail the occurrence of the homoclinic tangency to a periodic orbit for a thermokinetic model.[13] Within this framework we notice that our $P^{(n)}$ pulses can be identified with the fixed points P_n of the map representing the flow in the vicinity of the homoclinic reinjection detailed in the above references. In the most general case this map displays a very complex scenario consisting of period-doubling bifurcations which, however, gradually disappear as the dissipation is increased and the flow becomes strongly contracting. In fact, the situation with $a>1$ corresponding to Figs. 6(a) and 6(b) is characterized by a strong dissipation because of the long permanence of the system near $I=0$; this explains why period doubling is not observed but only a limited subdynamics corresponding to a mixture of $P^{(n)}$ regimes exists. Actually the disappearance of the true deterministic chaos for $a>1$ can be related just to the presence of such dissipation. In these conditions the noise plays a very important role by supplying the system with the fluctuations that in its deterministic counterpart are strongly damped. It really does not matter if the noise is very small but what is important here is that its action occurs precisely where the system is known to be strongly contracting, i.e., near $I=0$. Furthermore the noise is also instrumental in allowing us to visualize the shape of the unstable manifold in the vicinity of the reinjection region. As we can observe from Figs. 8(a) and 8(b), which represent the Poincaré section in a plane containing I_+, the portion of the map corresponding to the reinjection in Fig. 8(b) displays the same parabolic shape familiar in the analytical representation of the homoclinic tangency mechanism.[13] Situations where an enhancement of fluctuations occurs in laser systems have been analyzed by Arecchi *et al.*[28] whereas a first attempt to include noise in LSA equations is reported in Ref. 29.

In our system we identify the instability of the periodic solution as being of type I, i.e., with positive Liapounov numbers. This means that the stable manifold is homomorphic to the lateral surface of a cylinder as opposed to the type II where it is homomorphic to a Mobius strip (negative Liaupounov numbers);[13] furthermore in our case the unstable manifold of the periodic solution coincides with the corresponding two-dimensional manifold of I_+. An important property of the type-I homoclinic tangency is that all periodic windows appear on the same side of the limit point in a one-parameter space where transition $n-n+1$ accumulates, whereas in type II odd and even periods occur on oppo-

site sides. In the case of the LSA the limiting point of this sequence is necessarily the stationary regime I_+ and this explains why, as noticed above, chaos must always appear along the TL line, this one being also the line on which the homoclinic orbit must be found. As a matter of fact, by looking at Fig. 6(b) and focusing our attention in the region where the HB line and the TL line get closer, we notice that the order n of the pulses $P^{(n)}$ increases drastically as we move towards the TL line. The proximity of these two lines can also be understood in terms of the existence of the underlying homoclinic orbit based on an unstable cycle. In fact we notice that the stable manifold of this cycle forms the boundary separating the basin of attraction of I_+ and the set of orbits $P^{(n)}$. As A is increased the orbits $P^{(n)}$ and the boundary collide right on the TL line, a point of this line being characterized by a tangent collision, and the orbit drops on I_+. We observe numerically that the stable manifold is very sensitive to changes of A while the reinjection trajectory of the orbits $P^{(n)}$ suffers little modifications. The proximity of the HB and TL line can consequently be related to the rapidity with which the stable manifold grows as A increases, which is more true the more a is large.

As a next point we want to show that the chaotic regimes observed for $a<1$ are strongly connected with the existence of a limit cycle emerging from the Hopf bifurcation which undergoes period-doubling transitions. Figures 9(a) and 9(b) show the phase diagram in the space of the parameters $\bar{A}, A$ for a value of the saturability parameter $a=0.3$. The transition line TL and the HB delimit the region where bistability between I_+ and a variety of dynamical regimes, including chaotic ones, is observed. The unfolding of the bifurcations in the space of the parameters $\bar{A}, A$ reveals that for low values of A the T regime originated from supercritical Hopf bifurcation is stable and continuously transforms into $P^{(0)}$. As we move to higher values of A the HB turns subcritical and we observe a sequence of period doubling of the T regime. We observe continuous transitions also between re-

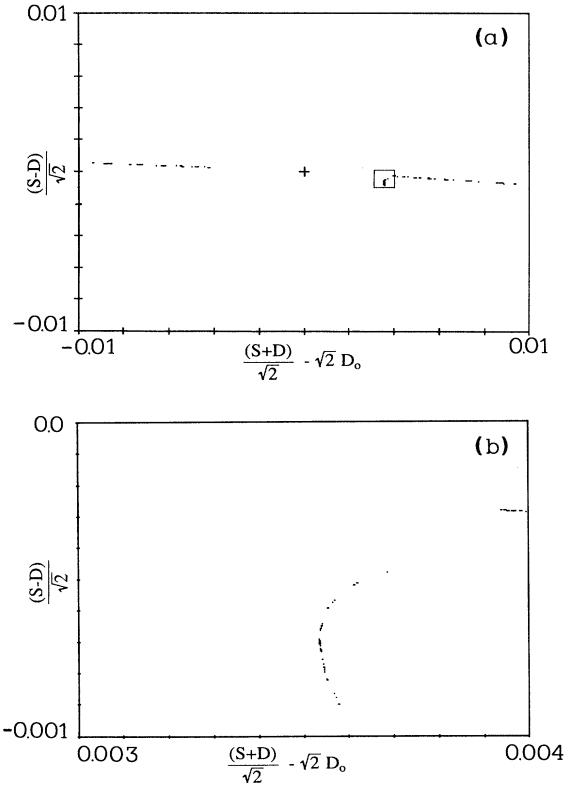

FIG. 8. Poincaré section in a plane perpendicular to the I axis containing I_+ (cross) for parameters $\bar{A}=1.1$, $A=5.7$. The origin coincides with I_+ and the x axis coincides with the bisector of the quadrant $D>0, S>0$. (b) is a blowup of the framed area in (a). The manifold on which the slow spiral-diverging motion takes place appears almost coincident with the x axis, while the parabola shaped reinjection structure is visible in the blowup (b). $D_0=S_0$ is the stationary value of D corresponding to I_+.

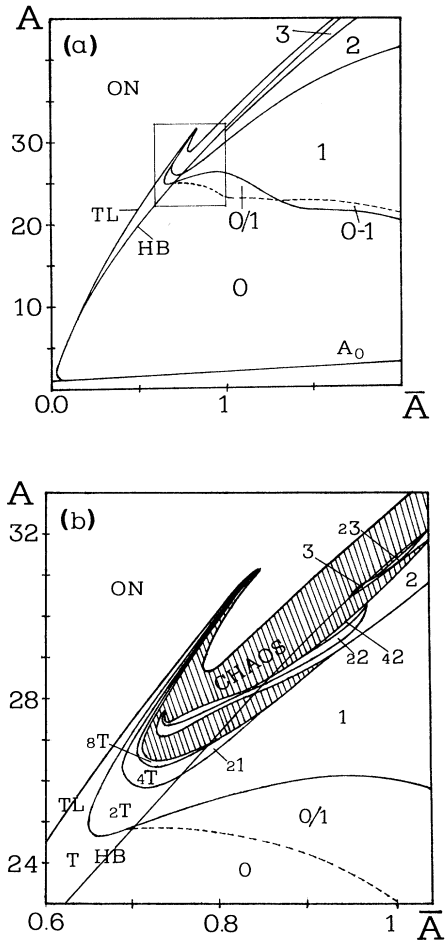

FIG. 9. State diagram of LSA in the space $\bar{A}, A$ for $a=0.3$. (a) Overall view. (b) Blowup of the inset in (a). 0/1 and 0−1 indicate, respectively, bistability and hesitation between $P^{(0)}$ and $P^{(1)}$ regimes. Period-doubling sequences appear for T regimes as well as for $P^{(2)}$ and $P^{(3)}$ regimes, these are prefixed by a small number denoting the order of the bifurcation sequence. Chaos occurs in the hatched area. Bistability of chaotic regimes with I_+ occurs between the HB and TL lines.

gimes $2T$ and $P^{(1)}$ and between $4T$ and $2P^{(1)}$. The period-doubling sequence can be observed up to the regime $8T$, after which we enter a region of chaotic behavior. Figure 10(a) shows a 3D portrait of the $2T$ regime while Fig. 10(b) shows a portrait of the chaotic attractor in a point of the chaotic region of Fig. 9(b). Embedded in the chaotic region shown in Fig. 9(b) there are windows of periodic regimes, $P^{(2)}$, $P^{(3)}$, and so on, they themselves undergoing a sequence of period-doubling bifurcations. We wish to draw attention to the hooklike shape of the transition line in Fig. 9(b) which surrounds the region where the lines corresponding to period-doubling bifurcations of the T regime accumulate. Moving down by keeping $\overline{A}$ constant and crossing this region can render the idea of the complexity of the branch of periodic solutions emerging from I_+. Initially we encounter the period-doubling sequence of T regimes leading to chaos, this suddenly disappears as we enter the region in which the only stable solution is I_+; by further decreasing A the chaotic region suddenly shows up again displaying a bistability with I_+. Finally we end by crossing regions of $P^{(n)}$ with relative inverse period-doubling sequence regimes until $P^{(0)}$ is reached. As a final consideration we notice that the overall phase diagram of Fig. 9(b) seems to be topologically equivalent to the experimental one of Ref. 2; however, one of the reasons for which no overlapping can be attempted is because the parameters used in the experiments, i.e., the cavity detuning and the absorber's pressure are different than those used in our simulations.

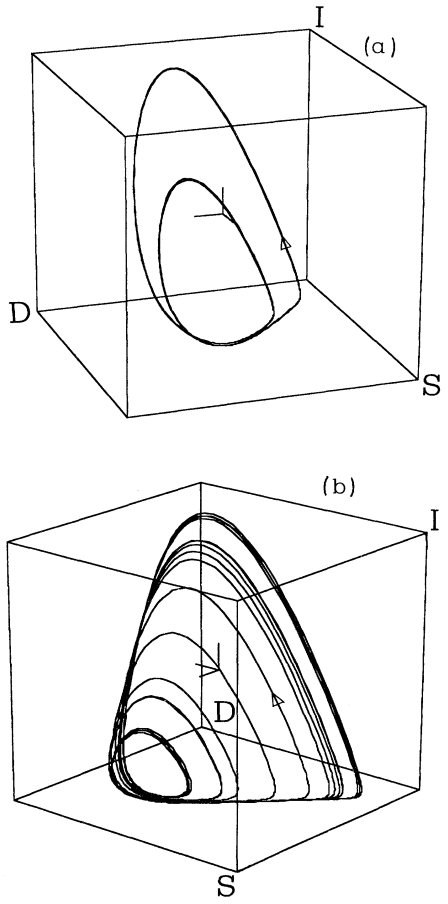

FIG. 10. Three-dimensional portraits of the $2T$ orbit for $\overline{A}=0.68$, $A=26$ with value ranges $D=S=(-0.09,-0.01)$, $I=(0,220)$ in (a); a few cycles of the chaotic attractor $\overline{A}=0.78$, $A=237$, with value ranges $D=S=(-0.09, -0.01)$, $I=(0,330)$ in (b).

As it appears the chaotic behavior in the case just discussed is much more complex than in the case of $a>1$; we believe that here also the instabilities have to be attributed to the presence of a homoclinic orbit biasymptotic to an unstable periodic solution. This is intuitively supported by the view of Fig. 10(b) where an unstable manifold and a reinjection process can be identified if the orbit portrait is carefully inspected. In addition the presence of period doubling on regimes $P^{(n)}$ is a mark for this kind of chaos. Further analysis in support of this idea, in particular, to evidentiate a reinjection structure getting close to the stable manifold of the saddle cycle as shown in Fig. 8 for the case $a>1$, is currently in progress.

E. Generalized bistability

An interesting case of bistability between the regimes $P^{(0)}$ and $P^{(1)}$ is also observed in the LSA. Contrary to the majority of the cases where transitions between $P^{(n)}$ regimes occur discontinuously or through hesitations here we observe the birth of a bistable behavior in the region between the dashed and the solid lines in Fig. 9. This is the only case of bistability between two stable periodic regimes that we have been able to detect. We note however that, while the transition appearing in the enlargements of Figs. 6(b) and 9(b) numerically obtained by increasing A have been determined quite accurately (about 400 points for each blowup), the occurrence of bistable situations has been checked less thoroughly only at the completion of the phase diagram. As a consequence of this some other bistability case may have passed undetected. It is interesting to notice how bistability between $P^{(0)}$ and $P^{(1)}$ transforms into a mixture of these two regimes as we move along the bistability region in Fig. 9(a).

V. CONCLUSIONS

We have studied systematically in the range of physically meaningful parameters a model for the LSA proposed by Tachikawa and co-workers. Our theoretical approach is much more general having the advantage of clearly evidencing the mathematical and physical structure of the model by depicting the relaxation processes with a set of time constants and coupling constants. In this framework we have pointed out a natural way to perform the adiabatic elimination of fast relaxation mechanisms as, for example, the rotovibrational relaxation in the amplifier medium, thereby making clear why the four-level models proposed in the past to investigate the LSA dynamics failed to display chaos. Furthermore the inclusion of additional relaxation processes as the very important one due to collisions with N_2 in the amplifier

medium, missed in the present model, should easily be taken into account and should produce significant modifications at the level of quantitative agreement with the experimental measurements. Some other important approximations have been carried out to describe the behavior of the absorber. Due to the high pressure in the absorbing cell in experimental situations a homogeneously broadened regime of absorption with a single absorbing line has been considered. However, these two approximations are not completely satisfied, for example, in CO_2-SF_6 LSA. In fact it is possible to estimate that a small amount of inhomogeneous broadening is present in the absorption; this would require the use of a Voigt profile to better describe this process. On the other hand, from preliminary calculations, in which the absorption factor in Eq. (14) has been replaced with the one in the full Doppler regime, we have been able to detect only negligible changes in the LSA behavior. With regard to the second approximation we believe that the presence of more than one absorbing line may be responsible for the anomalously high saturation intensity of the absorber attained in the LSA experiments. However, its inclusion in the LSA modeling would have required the knowledge of additional parameters of the absorber medium that are not available at the present. For these reasons, and even because the purpose of the present discussion was to firmly assess the scope of the existing models before attempting improvements, we have made the simplest choice of the LSA modeling.

We have found that the important parameter which determines the presence of chaotic behavior is the relative saturability of the absorber and this qualitatively agrees with experimental situations. In particular we have found that truly deterministic chaos occurs for $a < 1$ whereas when $a > 1$ the deterministic chaos occurs in an extremely small region of the space of parameters. In this context the presence of a very small noise, as spontaneous emission is, greatly amplifies the region in which random behavior is found. Furthermore the appearance of deterministic chaotic regimes when the relative saturability is smaller than unity indicates that the laser with a saturable absorber is a rather stable system whereas the laser with a saturable amplifier is a very unstable one. This statement should however be related only to the case of realistic laser parameters; it is, in fact, obvious that if a tends to zero the system becomes stable again.

With regards to a comparison with experiments and with data commonly used in the literature there is a serious discrepancy on the value of the amplification A as well on the saturability parameter a. On the other hand this model gives a good qualitative agreement with the pulse shapes and phase diagrams experimentally determined to lead one to trust it as a good model. We hope that this work will help to redeem the question either by a search of a better modeling or by an additional careful experimental verification.

We have investigated the nature of the chaotic regimes of the LSA and we have found that in order to acquire a better understanding of the onset of the chaotic regimes the branch of periodic solutions and proper Poincaré sections of the chaotic attractor must be considered. These, together with three-dimensional portraits of LSA orbits, led us to identify the homoclinic origin of the chaos in our laser system. In fact we have been able to ascertain the presence in our system of a homoclinic orbit biasymptotic to an unstable periodic motion of the system. This is of great importance in the LSA where previous analyses of this system attributed chaos to a homoclinic orbit biasymptotic to the unstable lasing stationary state. So far this last mechanism has received much attention in the field of laser instabilities, as opposed to the one that we have discussed for the LSA. We believe indeed that this mechanism, because of its transversal approach to the stable manifold of the stationary point, is by far more likely to occur in a given system than the homoclinicity to an unstable point where a longitudinal approach must occur.

ACKNOWLEDGMENTS

The author is greatly indebted to Professor E. Arimondo, Dr. F. Papoff, and Dr. D. Hennequin for continuous suggestions. and stimulating discussions. Furthermore, Professor J. V. Moloney and Dr. W. Forysiak are thanked for enlightening discussions on the branch of periodic solution in the LSA. This work was performed within the Dynamics of Nonlinear Optical Systems Twinning Program of the European Economic Community.

[1]D. Hennequin, F. de Tomasi, B. Zambon, and E. Arimondo, Phys. Rev. A **37**, 2243 (1988).

[2]A. Bekkali, F. Papoff, D. Dangoisse, and P. Glorieux, J. Phys. (Paris) Colloq. **49**, C2-349 (1988); D. Dangoisse, A. Bekali, F. Papoff, and P. Glorieux, Europhys. Lett. **6**, 335 (1988).

[3]E. Arimondo, F. de Tomasi, B. Zambon, F. Papoff, and D. Hennequin, J. Phys. (Paris) Colloq. **49**, C2-123 (1988).

[4]M. Tachikawa, F. L. Hong, K. Tanii, and T. Shimizu, Phys. Rev. Lett. **60**, 2266 (1988).

[5]E. Arimondo, F. Casagrande, L. A. Lugiato, and P. Glorieux, Appl. Phys. B **30**, 57 (1983).

[6]M. Tachikawa, T. Tanii, and T. Shimizu, J. Opt. Soc. Am. B **4**, 387 (1987).

[7]F. de Tomasi, D. Hennequin, B. Zambon, and E. Arimondo, J. Opt. Soc. Am. B **6**, 45 (1989).

[8](a) R. Salomaa and S. Stenholm, Phys. Rev. A **8**, 2695 (1973); **8**, 2711 (1973); Appl. Phys. **14**, 355 (1977); (b) D. E. Chyba, N. B. Abraham, and A. M. Albano, Phys. Rev. A **35**, 2936 (1987).

[9]M. Tachikawa, K. Tanii, M. Kajita, and T. Shimizu, Appl. Phys. B **39**, 83 (1986).

[10]D. Hennequin, M. Lefranc, A. Bekkali, D. Dangoisse, and P. Glorieux, in *Measures of Complexity and Chaos*, edited by N. B. Abraham, A. M. Albano, A. Passamante, and P. E. Rapp (Plenum, New York, 1990), p. 299.

[11]J. Y. Gao, H. Z. Zhang, X. Z. Guo, G. X. Jin, and N. B. Abraham, Phys. Rev. A **40**, 6339 (1989); Y. J. Kaufmann and U. P. Oppenheim, Appl. Opt. **13**, 374 (1974); E. Arimondo and E. Menchi, Appl. Phys. B **37**, 55 (1985).

[12]F. Argoul, A. Arneodo, and P. Richetti, J. Chim. Phys. **84**,

1367 (1987).
[13]P. Gaspard and X.-J. Wang, J. Stat. Phys. **48**, 151 (1987).
[14]B. Zambon, F. de Tomasi, D. Hennequin, and E. Arimondo, Phys. Rev. A **40**, 3782 (1989).
[15]P. Mandel and T. Erneux, Phys. Rev. Lett. **53**, 1818 (1984); C. Van Der. Brook and P. Mandel, Phys. Lett. A **122**, 36 (1987).
[16]F. T. Arecchi, W. Gadomsky, R. Meucci, and J. A. Roversi, J. Phys. (Paris) Colloq. **46**, C2-363 (1988); G. L. Oppo, J. R. Treddice, and L. M. Narducci, Opt. Commun. **69**, 393 (1989); F. T. Arecchi, W. Gadomsky, R. Meucci, and J. Roversi, *ibid.* **70**, 155 (1989).
[17]L. A. Lugiato, P. Mandel, S. T. Dembinski, and A. Kossakowski, Phys. Rev. A **18**, 238 (1978).
[18]K. Tanii, M. Tachikawa, M. Kajita, and T. Shimizu, J. Opt. Soc. Am. B **5**, 24 (1988).
[19]H. G. Van Kampen, *Stochastic Processes in Physics and Chemistry* (North-Holland, Amsterdam, 1981), Chap. V.
[20]H. Haken, Phys. Lett. **53A**, 77 (1975); L. M. Narducci, H. Sadiky, L. A. Lugiato, and N. B. Abraham, Opt. Commun. **55**, 370 (1985).
[21]P. Mandel and T. Erneux, Phys. Rev. A **30**, 1893 (1984); **30**, 1902 (1984).
[22]U. P. Oppenheim and P. Melman, IEEE Quantum Electron. **QE-426**, 426 (1971).
[23]R. D. Hampstead and M. Lax, Phys. Rev. **161**, 350 (1967); M. Lax and W. H. Louisell, *ibid.* **185**, 568 (1969).
[24]J. V. Moloney, J. S. Uppal, and R. G. Harrison, Phys. Rev. Lett. **59**, 2868 (1987); W. Forysiak, R. G. Harrison, and J. V. Moloney, Phys. Rev. A **39**, 421 (1989); J. V. Moloney, W. Forysiak, J. S. Uppal, and R. G. Harrison, *ibid.* **39**, 1277 (1989).
[25]T. Erneux, J. Opt. Soc. Am. B **5**, 1063 (1988).
[26]J. Guckenheimer and P. Holmes, *Nonlinear Oscillations, Dynamical Systems and Bifurcations of Vector Fields* (Springer, Berlin, 1984); L. Shil'nikov, Sov. Math. Dokl. **6**, 163 (1965); J. Neimark and L. Shil'nikov, Sov. Math. Dokl. **6**, 305 (1965).
[27]L. Shil'nikov, Math. Sb. **10**, 91 (1970); N. K. Gavrilov and L. P. Shil'nikov, Math. SSSR Sb. **17**, 467 (1971); **19**, 139 (1973).
[28]F. T. Arecchi, W. Gadomsky, A. Lapucci, H. Mancini, R. Meucci, and J. A. Roversi, J. Opt. Soc. Am. B **5**, 1153 (1988).
[29]D. Hennequin, F. De Tomasi, L. Fronzoni, B. Zambon, and E. Arimondo, Opt. Commun. **70**, 253 (1989).